RSC Advances

ROYAL SOCIETY OF CHEMISTRY

www.rsc.org/advances

Journal Name

ARTICLE

Effects of Organic Additives on the immersion gold depositing from a Sulfite-Thiosulfate Solution in an Electroless Nickel immersion gold Process

Received 00th January 20xx,
Accepted 00th January 20xx

DOI: 10.1039/x0xx00000x

www.rsc.org/

Yao Wang[a], Haiping Liu[a], Sifu Bi[b], Mengxue He[a], Chunyu Wang[b], Lixin Cao[a]*

An immersion gold-plating process on electroless Ni-P alloy substrate was investigated. The immersion Au coating was deposited from a thiosulfate-sulfite mixed ligand bath based on Ni-P alloy substrate. The effects of three organic additives, such as polyethylenimine (PEI), hexamethylene tetramine (HET) and benzotriazole (BTA) on the depositing process and the performance of Au coating were investigated. The study was performed by measuring the open circuit potential-time curves in situ and Tafel tests in combination with X-ray fluorescence spectrometry (XRF), scanning electron microscope (SEM), Raman spectroscopy and X-ray diffraction (XRD) analysis techniques. The results show that PEI, HET and BTA could adsorb and desorb on the surface of Au coating and they had the similar influences on the open circuit potential. With these organic compounds adding, the plateau potential shifts to the positive direction, and the time for the potential to reach the plateau value decreases with increasing additive concentration. The XRF, XRD and SEM studies indicated that these three additives decreased the initial deposition rate, decreased the size of Au particles, and thus changed the morphology of Au deposits. Tafel studies demonstrated that the corrosion resistance of Au coating could be improved by adding PEI, HET or BTA to immersion gold bath. A cause for understanding these additives was indicated based on the above experiments.

1. Introduction

Electroless nickel/immersion gold (ENIG) process plays a great part in the microelectronics field as a final finish[1-3]. The ENIG films are extensively applied in Printed Circuit Boards (PCBs) because of its excellent electrical conductivity, planarity, good solderability, and corrosion resistance[4-8]. The cyanide gold plating containing potassium dicyanoaurate ($KAu(CN)_2$), as the source of gold in the immersion gold (IG) bath, has been widely used to obtain gold coating on Ni-P alloy substrate due to its outstanding advantages, such as the bath stability and the superior performance of the obtained coating[9]. However, the development of cyanide is gradually limited owing to the toxicity and material compatibility problems[10]. Therefore, considering the safety and the demands for manufacture, the researchers attempt to develop a non-cyanide bath[11]. Yurong Wang[12] reported that Au coating prepared from a non-cyanide bath containing Choline chloride and chloroauric acid ($HAuCl_4$) possessed good properties on solderability and corrosion resistance. Furthermore, Au (I)-sulfite complex and Au (I)-thiosulfate complex are also used for non-cyanide gold plating respectively[13]. Compared with only one ligand in the IG bath, the gold solution used thiosufate and sulfite as the mixture lighands has a better stability. Moreover, it was also reported that the thiosulfate-sulfite mixture itself in the IG bath was a reducing system and the sulfite played a main role as reducing agent[14].

Immersion gold process can be considered as a controlled corrosion process that nickel atoms on the surface of the Ni (P) substrate are replaced by gold atoms[15]. A hyperactive corrosion of Ni-P coating takes place during the IG process which has been named for the "black pad" phenomenon[16-21], resulting in a failure with joint integrity for wire bonding and soldering after assembly[22]. Corrosion properties of Ni-P alloy substrate are influenced by the operating parameters of ENIG process such as phosphor content, pH value, temperature, etc [5, 6, 21, 23]. It was also reported that some trace amounts of organic compounds, such as polyethylenimine (PEI)[24], thiourea (TU)[25], and 3-S isothiuronium propyl sulfonate (UPS)[26] have influence on the electroless nickel coating or gold film. So, it is meaningful to study the immersion gold process and the performance of Au coating during the IG process with different organic additives.

In this study, we added three organic compounds, polyethylenimine (PEI), hexamethylene tetramine (HET) and benzotriazole (BTA) to the thiosulfate-sulfite mixed ligand bath, and investigated the effects of these additives on the deposition process. Furthermore, we have studied the changes of the morphology, structure of the gold films deposited from the IG bath with different additives. Meanwhile, with the help of electrochemical method, the effect of these three additives on Au films corrosion resistance was investigated and discussed.

2. Experimental

2.1. Materials and methods

[a] School of Marine Science and Technology, Harbin Institute of Technology, Weihai 264209, China
[b] School of Materials Science and Engineering, Harbin Institute of Technology, Weihai 264209, China Address here.
*E-mail: hpliuhit@126.com

Copper sheets with dimension of 20 mm×20 mm×0.25 mm were plated by typical ENIG process including electroless Ni-P alloy, followed by immersion Au deposition. Before electroless plating, the Cu substrate was prepared by a series of pretreatment procedures. Palladium solution was used to activate the Cu substrate in order to the subsequent EN plating. After rinsing in distilled water, the freshly plated Ni-P samples (about 11.0% P) were immediately immersed into the gold bath for 10 min to obtain the gold coating. All the solutions and ENIG steps were prepared with distilled water. Chemical composition and typical process parameters for IG plating are shown in Table 1.

Table 1 Composition and operation condition of IG

Chemicals	Concentration (g/L)	condition
$Na_3Au(SO_3)_2$	2 g/L	
Na_2SO_3	8 g/L	
$Na_2S_2O_3$	60 g/L	
Buffering agent	50 g/L	
Temperature		80±2℃
pH		6.0
Immersion time		10 min

2.2. Characterization of the coatings

The thickness of Au coating with different additives in the IG bath was carried out by X-ray fluorescence (XRF, BrukeraxsS4 Explorer, Germany). The XRF spectra were evaluated by the automatic analysis program Spectraplus. The deposition rate was calculated based on the relationship between Au film thickness and deposition time. Scanning electron microscope (SEM) was used to analyze the surface morphology of specimen. The Raman spectra (3600-500cm^{-1}) was measured on Renishaw Invia with a resolution of 2cm^{-1}. Meanwhile, X-ray diffraction (XRD) using Cu Kα radiation, 2θ from 35°to 85°was performed to investigate the crystal structure of ENIG coating.

2.3. Electrochemical measurements

Electrochemical measurements mainly consisted of open circuit potential (OCP) measurement and Tafel curve tests using a CHI electrochemical station (model 660E) with a traditional three-electrode system including a working electrode, a reference electrode and a counter electrode. The reference electrode was a saturated calomel electrode (SCE), and the counter electrode was a platinum plate. A Luggin capillary was placed near the working electrode to minimize the solution resistance. For both open circuit potential measurement and Tafel tests, the Cu substrate was first sealed using insulated adhesive tape, except for a 2×2 cm effective working area, followed by EN deposition. After cleaning in deionized water, the samples were rapidly immerged into the gold solution as working electrodes for the open circuit potential measurement in situ. To minimize the influence of the Au coating thickness on electrochemical measurement parameters, all the samples were deposited to have a similar thickness of about 0.3 μm. The Tafel tests for the coated films were carried out at room temperature in a 3.5% NaCl solution. Prior to the beginning of Tafel measurements, the specimens were dipped in the ethyl alcohol for 1 min to remove the oil, kept in the 3.5% NaCl solution for 15 min to stabilize the potential, and this potential was then taken as the open circuit potential. The potential test range was E_{OCP} ± 300 mV with a rate 5 mV/s. According to the results of Tafel fitting, the corrosion parameters of Au coating were calculated.

3. Results and discussion

3.1. Open circuit potential-time curves in situ

Fig. 1 (a)-(c) reveals the open circuit potential-time curves of electroless Ni-P substrate during the immersion gold process from a sulfite-thiosulfate solution with three organic additives. It is clearly seen that in all the curves, the open circuit potential-time curves are similar. Thus, the potential firstly positive shifts, and then, within a short time, the potential attains a steady plateau. In addition, in the presence of additives, the plateau potential shifts to the positive direction, and the time for the potential to reach the plateau value decreases, showing that the effects of different additives on the electrode state are similar. Furthermore, with increasing additives concentration from IG bath, not only the plateau potential shifts to the positive direction, but also the time reaching the plateau potential value gets shorter. However, the plateau potential has a negative shifting, when further increasing additives concentration to be a high value, such as 400 mg/L PEI, 10 mg/L HET and 4 mg/L BTA. Note that the plateau potential of 3 mg/L BTA (about -0.11V) is more positive than that of the other two additives, such as 300 mg/L PEI and 7 mg/L HET (about -0.17V), which indicates that BTA has a more obvious influence on the plateau potential.

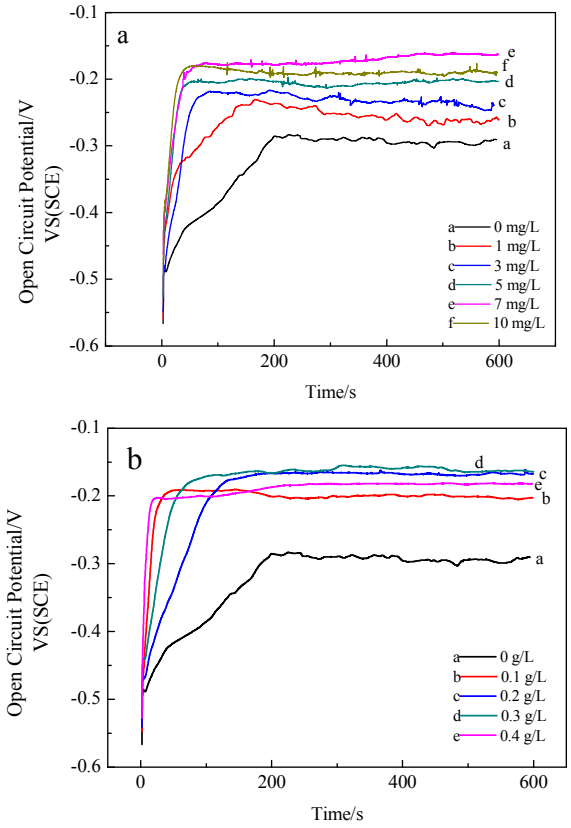

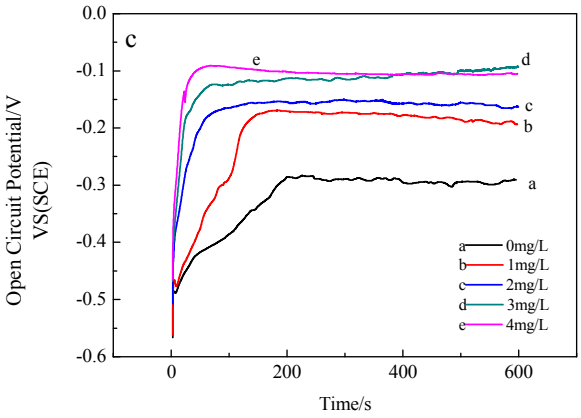

Fig. 1 Open circuit potential-time curves of immersion gold with different concentration of additives. (a) HET, (b) PEI, (c) BTA.

According to our previous study[5], the variations in open circuit potential and deposition rate during the IG process could reflect the changes of the electrode surface state. As the gold deposition proceeds, the EN electrode surface is gradually covered by the gold layer, resulting in a positive shifting of potential. As the gold deposition continues, the potential attains the plateau value due to the formation of gold deposit on the surface of Ni substrate. Note that, in the presence of additives, the plateau potential is more positive, which indicates that gold film has an increasing coverage on the Ni-P alloy. Moreover, the time for the potential to reach the plateau value corresponds to the time for formation of gold film on the Ni-P substrate gets shorter. Larger coverage with less time states that these additives in the bath could lead to a uniform and compact gold layer, which could offer a better protection for Ni substrate.

3.2. Immersion gold deposition rate-time curves

Fig. 2 presents the gold deposition rate-time curves of Au layer during the IG process with different additives analyzed by XRF analysis. As can be seen from Fig. 2, the variation of deposition rate with time is similar. The initial deposition rate often has a higher value, and then deposition rate decreases with time. Furthermore, a lower initial deposition rate could be obtained at an initial stage in the presence of the three organic additives. However, all the additives could hardly affect the subsequent gold deposition rate.

It's noted that the changes in deposition rate and electrode potential during IG process are related to the variations of the electrode surface state. As the Ni-P substrate begins immersing in the IG bath, Au^{+}-Ni galvanic cell is formed on the Ni electrode surface. In this case, the potential difference as driving force of immersion gold[27] is the maximum, and the deposition rate reaches the fastest. As the gold deposition proceeds, Ni surface is gradually replaced by the gold films. Thus, the potential difference diminishes along with a decrease of the deposition rate. At the last stage of gold deposition, Ni surface is completely covered by gold layer, and the deposition rate is relatively low.

According to the mechanism of immersion plating[2], the deposition rate of Au coating could be equal to the corrosion rate of Ni film. So, the lower rate at initial stage with additives indicates that the corrosion rate of Ni substrate is also reduced, which could be explained by two factors. On one hand, a lower deposition rate promotes the nucleation, forming a dense Au crystal with fine protection on Ni-P alloy. On the other hand, organic additives could adsorb on the active sites of EN films, selectively, resulting in the uniform distribution of active components on the Ni-P film and hence avoiding the over-corrosion of Ni-P alloy during the IG process. This result agrees with our previous studies that PEI could decrease the corrosion of Ni substrate during the IG process. Furthermore, in the later stage of gold deposition, Ni surface is almost covered with gold layer. The absorption of additives decreases or even disappears, resulting in a less impact on the following rate of immersion gold plating.

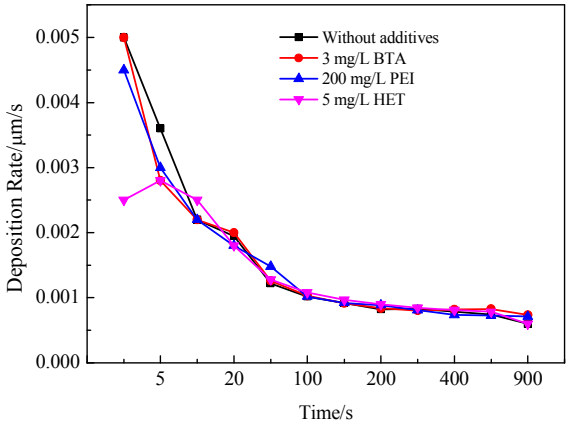

Fig. 2 Deposition rate-time curves of immersion gold with different additive.

3.3. The morphology of Au deposit

Fig. 3 shows the typical morphology of the IG deposit with and without additives. The surface of gold coating from the IG bath without additives shows a porous surface with uneven distribution of pits. A honeycomb structure is observed in the presence of 200 mg/L PEI. Moreover, the honeycomb structure becomes more evident with an addition of 3 mg/L BTA.

It is known that the initial growth of gold deposition includes the forming and the growth of nucleus. The growth begins at certain active sites, and continues isotropous resulting in hemispherical islands of Au. New grains will grow if the size of an initial cluster exceeds critical dimension. We presume that this difference of surface may be related to the influence of the three additives on the growth of island.

The chemical structures of additives are shown in Fig. 4. These three additives may be classified as an organic corrosion inhibitor which containing nitrogen element. The nitrogen atoms as the adsorption centre interact with metal surface. In BTA structure, it also has the unsaturated π electron to coordinate with metal[28]. Furthermore, some studies[29] have reported that BTA inhibits the corrosion of the composite by adsorbing physically onto the surface of metal, resulting in a strong adsorption on the metal surface. Thus, this special adsorption mode of BTA may make the honeycomb morphology more obvious and the most positive plateau potential of 3 mg/L BTA may be related to this special adsorption as well.

3.4. XRD analysis of the ENIG coating

The XRD patterns of ENIG coating with and without additives are shown in Fig. 5. As can be seen that the crystal structure and composition in different samples are agreed well with others reports[30]. There is no obvious change in the crystalline phase of ENIG coating with and without additives from the patterns. The diffraction peaks of Cu could be seen because of a thin layer of Au cover. The peaks of Cu (111), Cu (200) and Cu (220) around 2θ of 43°, 50.5°and 74°are observed, and the Au (111), Au (220) and Au (311) phases are detected at 38.5°, 65° and 77.5°, respectively.

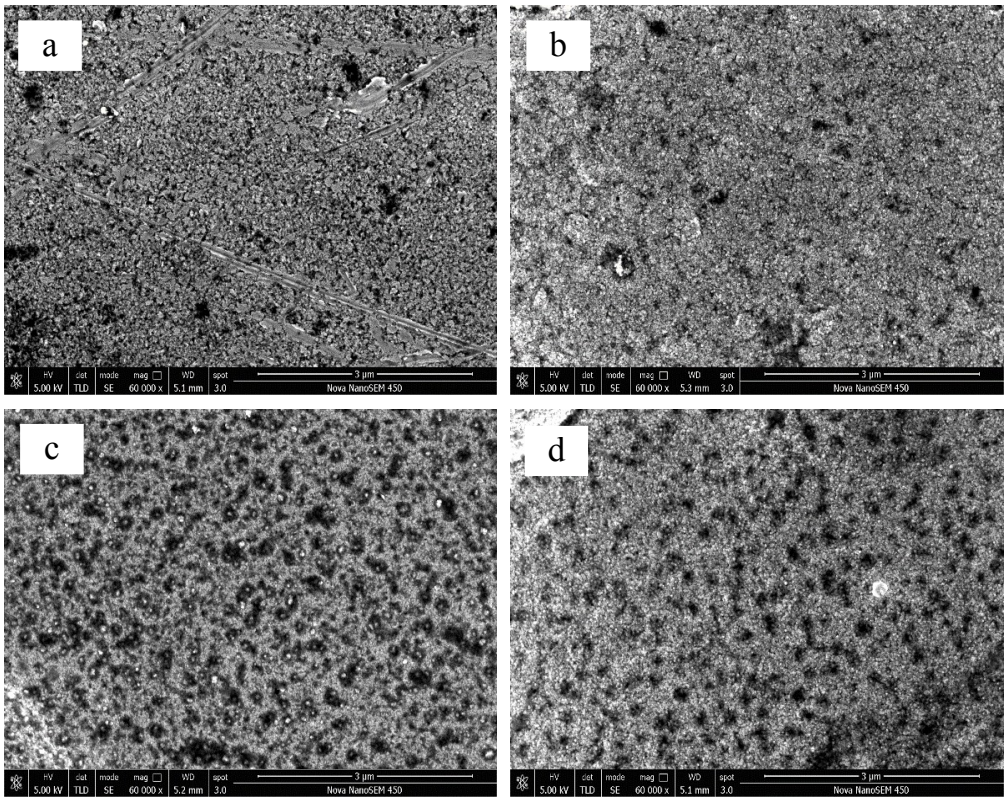

Fig. 3 SEM images of Au coating with different additive in the bath. (a) Without additive, (b) 200 mg/L PEI, (c) 3 mg/L BTA, (d) 5 mg/L HET

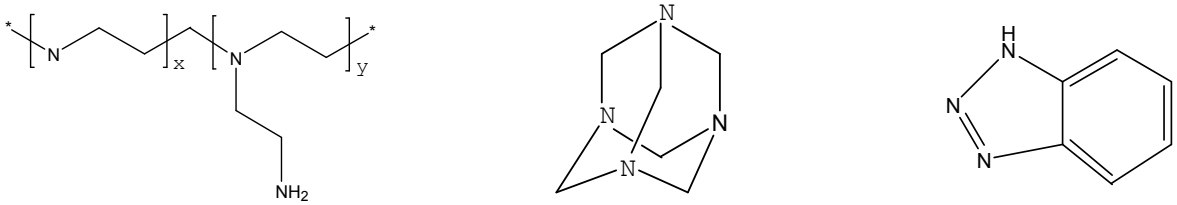

Fig. 4 The chemical structures of additives

Table 2 The average grain size of Au coating in different specimens

Additive	Without additive	3 mg/L BTA	200 mg/L PEI	5 mg/L HET
Average grain size (nm)	25.4	22.6	22.7	15.6

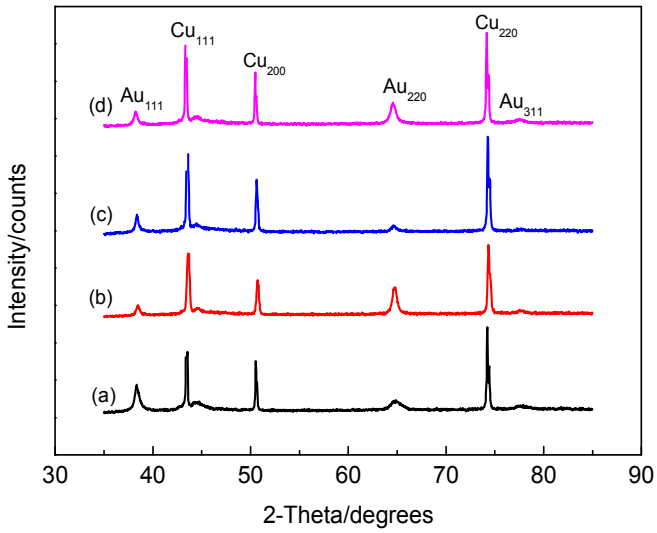

Fig. 5 XRD patterns of ENIG coating with different additives. (a)Without additive, (b)5 mg/L HET, (c)200 mg/L PEI, (d)3 mg/L BTA.

Furthermore, the average grain size of Au coating using the fitting of diffraction peak and Debye-Scherrer equation[12] is estimated (shown as Table 2). According to Table 2, in the presence of additives, the average grain size of Au coating decreases. The reason of decrease of average grain size of Au may be that the additives may promote Au crystal formation during the process of gold deposition and the number of grain per unit volume increases.

3.5. Raman spectra analysis of the Au coating

The Raman spectra of Au coating with and without additives were shown in Fig. 6. These three organic additives all have the same nitrogen functional groups. However, there is no Raman band at about 3400cm^{-1} corresponding to N-H stretching. Furthermore, in the spectra of BTA, the signal at about 1440cm^{-1}(N=N stretching) is not observed. Based on the above results, it can be concluded that the additives could adsorb and desorb on the surface of Au coating.

3.6. Electrochemical corrosion study

To obtain more supports for the mentioned that organic additives could improve the quality of gold layer, polarization curves are used to evaluate corrosion resistance of Au coating. Fig. 7 shows the Tafel curves of Au coating with and without additives in 3.5% NaCl solution at room temperature. The corresponding parameters, such as corrosion potential (E_{corr}), corrosion current (I_{corr}), anodic transfer coefficient (β_a), cathodic transfer coefficient (β_c) were calculated by the Tafel curves using a CHI electrochemical station. The corresponding values were given in Table 3. In addition, the polarization resistance (R_p) and the total coating porosity (P) were calculated according to the following equations[31, 32]:

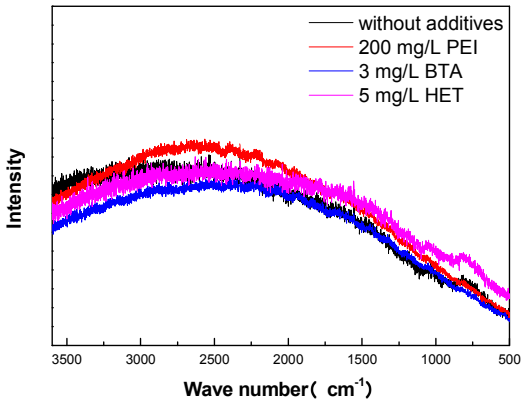

Fig. 6 Raman spectrum of Au coating with and without additives

Table 3 Corrosion properties of ENIG film with different additive.

Samples(ENIG)	E_{corr}(V)	I_{corr} ($\mu A/cm^2$)	β_a (V/decade)	β_c (V/decade)	R ($\Omega \cdot cm^2$)	P (%)
Ni-P substrate	-0.495	19.59	0.0343	0.0199	2795	
Without additive	-0.413	21.51	0.0175	0.0127	1487	7.64×10^{-1}
5 mg/L HET	-0.278	5.89	0.0184	0.0185	6809	1.94×10^{-5}
3 mg/L BTA	-0.293	3.254	0.0136	0.0209	11008	3.28×10^{-5}
200 mg/L PEI	-0.392	8.71	0.0222	0.0159	4625	6×10^{-2}

$$R_p = \frac{\beta_a \times \beta_c \times 10^7}{2.3 \times i_{corr} \times (\beta_a + \beta_c)} \quad (1)$$

$$P = \frac{R_{pm(substrate)}}{R_{p(coating-substrate)}} \times 10^{-\left|\Delta E_{corr} / \beta_{a(substrate)}\right|} \quad (2)$$

R_p is the polarization resistance, P the total coating porosity, R_{pm} the polarization resistance of the substrate, ΔE the corrosion potential difference between the coating and Ni-P substrate, and β_a and β_c are the anodic and cathodic Tafel slopes for the samples, respectively. The corrosion data is also summarized in Table 3.

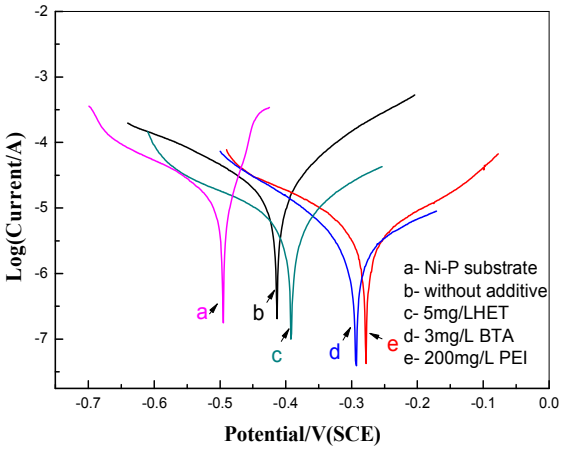

Fig. 7 Tafel curves of Au coating deposited from the bath with different additive. (a)Ni-P substrate, (b)Without additive, (c)5 mg/L HET, (d) 3 mg/L BTA, (e)200 mg/L PEI.

As can be seen in Fig. 7, the results of Tafel tests indicate a similar trend in the corrosion behaviors of ENIG coating with different additives. All three ENIG coatings with additives have a more positive corrosion potential (E_{corr}) and lower corrosion current (I_{corr}) than the coating without, which illustrates that with the help of additives, the gold film had a better corrosion resistance. In addition, the comparison of the porosity of different samples (Table 3) indicates that all the gold coatings with these three additives had lower porosity, and the porosity of coating with addition of HET and BTA is relatively lower. Combined the Tafel tests results with the open circuit potential measurements, it can be concluded that BTA has a better corrosion inhibition effect among additives.

4. Conclusion

The results show that PEI, HET and BTA have similar effect on the depositing process and the performance of Au coating. They could adsorb and desorb on the surface of Au coating and BTA has a better corrosion inhibition effect. In the presence of additives, the plateau potential positive shifts, accompanied with a decrease of initial deposition rate, and the time reaching the plateau potential value becomes shorter with increasing additive concentration. In addition, according to the SEM and XRD results, the morphology of immersion gold surface shows a honeycomb structure and the size of Au particles gets smaller. Furthermore, Tafel tests carried out in 3.5% NaCl solution indicated that Au coating with additives has a higher corrosion resistance and lower porosity.

Acknowledgements

This work was funded by an NSFC Grant (No. 51301052 and 21273056) supported through the NSFC Committee of China.

Notes and references

1 R. K. Sharma, R. Kaneriya, S. Patel, A. Bindal and K. C. Pargaien, *Microelectron Eng*, 2013, **108**, 45-49
2 D. Lee and H. S. Lee, *Microelectron Rellab*, 2006, **46**, 1119-1127.
3 D. Lee, S. Huh, C. Kim, S. Mun, H. Shin and H. Lee, *Electron Mater Lett*, 2015, **11**, 695-701.
4 S. Gao, Z. Chen, A. Hu, M. Li and K. Qian, *J Mater Process Tech*, 2014, **214**, 326-333.
5 H. Liu, N. Li, S. Bi and D. Li, *J Electrochem Soc*, 2007, 154, D662.
6 G. Cui, J. Zhao, S. Liu and G. Wu, *The Journal of Physical Chemistry* , 2011, **115**, 21169-21176.
7 M. Bacior, N. Sobczak, A. Siewiorek, A. Kudyba, M. Homa, R. Nowak, M. Dziula and S. Masłoń, *J Mater Eng Perform*, 2015, **24**, 754-758.
8 J. Wojewoda-Budka, Z. Huber, L. Litynska-Dobrzynska, N. Sobczak and P. Zieba, *Mater Chem Phys*, 2013, **139**, 276-280.
9 T. N. Vorobyova, S. K. Poznyak, A. A. Rimskaya and O. N. Vrublevskaya, *Surface and Coatings Technology*, 2004, 176, 327-336.
10 J. Sato, M. Kato, H. Otani, T. Homma, Y. Okinaka, T. Osaka and O. Yoshioka, *J Electrochem Soc*, 2002, **149**,C 164.

11 J. Sato, M. Kato, H. Otani, T. Homma, Y. Okinaka, T. Osaka and O. Yoshioka, *J Electrochem Soc*, 2002, **149**, C168.
12 Y. Wang, X. Cao, W. Wang, N. Mitsuzak and Z. Chen, *Surface and Coatings Technology*, 2015, **265**, 62-67
13 Y. Hoshino and O. Masao, *Gold Bull*, 1998, **31**, 1.
14 M. Kato and Yutaka Okinaka, *Gold Bull*, 2004, **37**, 37-44.
15 R. J. Coyle, D. E. H. Popps, A. Mawer, D. P. Cullen, G. M. Wenger and P. P. Solan, *IEEE Transactions on Components and Packaging Technologies*, 2003, **26**, 724-732.
16 K. H. Kim, J. Yu and J. H. Kim, *Scripta Mater*, 2010, **63**, 508-511.
17 K. Zeng, R. Stierman, D. Abbott and M. Murtuza, *JOM-US*, 2006, **58**, 75.
18 M. N. Collins, J. Punch and R. Coyle, *Solder and Surf Mt Tech*, 2012, **24**, 240-248.
19 Y. S. Won, S. S. Park, J. Lee, J. Kim and S. Lee, in *Applied Surface Science*, 2010, vol. 257, pp. 56-61.
20 Y. S. Won, S. S. Park, J. Lee, J. Kim and S. Lee, in *Applied Surface Science*, 2010, vol. 257, pp. 56-61.
21 Rimantas Ramanauskas, A. Selskis, J. Juodkazyte and V. Jasulaitiene, *Circuit World*, 2013, **39**, 124-132.
22 Kejun Zeng, R. Stierman and D. Abbott, *The Tenth Intersociety Conference on. IEEE,* 2006, 1111-1119.
23 T. S. N. Sankara Narayanan, I. Baskaran, K. Krishnaveni and S. Parthiban, *Surface and Coatings Technology*, 2006, **200**, 3438-3445.
24 K. Suda, Y Ohya and Y Takizawa, U.S.Patent, 2003, 6,736,886.
25 H. Liu, N. Li, S. Bi, D. Li and Z. Zou, *Thin Solid Films*, 2008, **516**, 1883-1889.
26 H. Liu, S. Bi and N. Li, *Russ J Eelectrochem*, 2009, **46**, 383-388.
27 R. F. Champaign, Jodi. A. Roepsch and M. R. Downey, *Journal of Surface Mount Technology*, 2002, **15(3)**, 19-24.
28 O. Hollander, R.C. May, *Corrosion*, 1985, **141,** 39–45.
29 Han, Y, D. Gallant and X.G. Chen, *Materials Chemistry and Physics*, 2013. **139(1)**, 187-195.
30 Q. V. Bui, N. D. Nam, D. H. Choi, J. B. Lee, C. Y. Lee, A. Kar, J. G. Kim and S. B. Jung, *Mater Res Bull*, 2010, **45**, 305-308.
31 S. H. Ahn, J. H. Lee, H. G. Kim and J. G. Kim, *Appl Surf Sci*, 2004, **233**, 105-114.
32 N. D. Nam, J. G. Kim and W. S. Hwang, *Thin Solid Films*, 2009, **517**, 4772-4776.